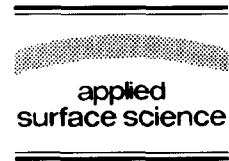




ELSEVIER

Applied Surface Science 96–98 (1996) 352–358



# Laser beam application to thin film transistors

T. Sameshima \*

*Tokyo University of Agriculture and Technology, Koganei, Tokyo 184, Japan*

Received 22 May 1995

---

## Abstract

Laser crystallization and amorphization of silicon films are discussed. Poly-Si films with fine crystalline grains ( $< 100$  nm) are formed by liquid/solid interface controlled growth with a velocity of 0.6 m/s by a XeCl excimer laser irradiation. Large grain growth of silicon films ( $> 1 \mu\text{m}$ ) is also discussed. An amorphous state is achieved via rapid solidification when silicon films are melted completely. Crystallization and amorphization are reversible. They are governed by the laser energy density. The application of the rapid laser heating method to fabrication of top-gate-type poly-Si and a-Si thin film transistors (TFTs) is discussed. TFTs with a high mobility,  $620 \text{ cm}^2/\text{Vs}$  (poly-Si) and  $2.6 \text{ cm}^2/\text{Vs}$  (a-Si) were achieved by a  $270^\circ\text{C}$  fabrication process. Application of a laser-induced-forward transfer to TFT fabrication is proposed for a simple process with a low cost.

---

## 1. Introduction

The pulsed-laser-induced rapid heating method has been applied to fabrication of thin film semiconductor devices, especially, polycrystalline silicon thin film transistors (poly-Si TFTs) [1–5]. Crystallization of silicon films and activation of dopant are achieved without heating substrates to a high temperature. Good crystallized films with a high carrier mobility are realized. These characteristics of the pulsed laser heating method are suitable for a low temperature processing. For example, it allows an usage of a cheap glass as a substrate, on which switching transistors are fabricated for liquid crystal display (LCD) devices. The pulsed laser induced melting of silicon thin films also allows amorphization of thin silicon films [6,7]. Amorphization occurs for irradiation with

higher energies than the energies required for crystallization. It is therefore important to control the laser energy to get good crystalline films for the TFT application.

This paper first discusses characteristics of laser induced crystallization and amorphization of silicon films. It then reports an application of the laser heating method to fabrication of polycrystalline and amorphous (poly-Si and a-Si) TFTs at a low temperature ( $< 300^\circ\text{C}$ ). It is demonstrated that the formation of a good  $\text{SiO}_2/\text{Si}$  interface is essential for fabricating TFTs with high performances. This paper also discusses an application of laser ablation to TFT fabrication processing.

## 2. Pulsed laser-induced melting of silicon films

Fig. 1 shows threshold energies for crystallization and amorphization as a function of the film thick-

---

\* Corresponding author. Tel.: +81-423-88-7109; fax: +81-423-85-6729; e-mail: tsamesim@cc.tuat.ac.jp.

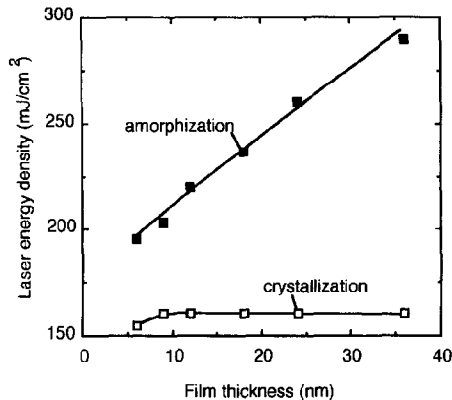


Fig. 1. Threshold energies for crystallization and amorphization as a function of film thickness. Initial materials were a-Si:H deposited on quartz substrate. A 30 ns pulsed XeCl excimer laser was used.

ness. Hydrogenated amorphous silicon (a-Si:H) films formed on quartz substrates were melted by irradiation with 30-ns-pulsed XeCl excimer laser with an energy above surface melting threshold of 160 mJ/cm<sup>2</sup> and a liquid-solid interface is formed in the films. The threshold energy for crystallization was almost independent of the film thickness because the most of the heating energy produced in silicon films by irradiation diffuses into the quartz substrate until the silicon surface is heated to the melting temperature. After irradiation, the liquid/solid interface moves toward the surface through heat diffusion into the substrate. The speed of the interface is governed by heat diffusion. It was experimentally determined as 0.6 m/s using transient conductance for 20 nm thick silicon films [7]. Crystallization occurs along the direction of interface movement to the surface. Crystalline grains can grow spherically from nucleation sites located near the Si/quartz interface in the initial stage of melting (interface controlled growth). The grain growth is then limited by the film thickness and the melt duration.

The crystalline grain size increases as the laser energy increases. Transmission electron microscopy (TEM) measurement revealed that 30 nm thick silicon films crystallized with a laser energy of 240 mJ/cm<sup>2</sup> had grain size no more than 60 nm. On the other hand, Kuriyama et al. made crystalline films with grains larger than 1 μm using hundred laser

pulses with a help of substrate heating (~450°C), which enhanced grain growth in the lateral direction [8]. Im et al. reported an interesting grain growth larger than 1 μm, which is achieved by a single pulse irradiation with an energy just below the amorphization threshold without heating the substrate [9]. In Im's condition, the films are almost melted throughout the film thickness so that the density of the crystalline nucleation is reduced and rapid crystallization in the lateral direction is caused by a large difference of the free energy between the liquid silicon and the solid silicon at the solidification point. Furthermore, we also observed that large grain growth, 1.2 μm × 0.5 μm, when patterned silicon islands with a size of 10 μm × 40 μm and a thickness of 70 nm were melted completely by irradiation with an energy of 360 mJ/cm<sup>2</sup> [10]. When silicon islands formed on quartz substrates were melted completely by irradiation, the film shape was changed into a globular shape due to surface tension. The area shrank from edges by a size of 3.3 μm and the thickness increased to 270 nm at the edge regions. The heat diffusion was reduced and thermal energy was piled up in liquid silicon at the edge regions during the melting. This resulted in an increment of melt duration to 400 ns and a reduction of the cooling rate to 2 × 10<sup>9</sup> K/s at the edge, while the melt duration was short, 170 ns, and the cooling rate was high, 6.5 × 10<sup>9</sup> K/s at the middle region in the island. A temperature gradient was therefore caused in the lateral direction and an interface controlled growth in the lateral direction was occurred. The crystalline grains were lined in two deep along the length of the islands. The position of grains in the direction of grain length were defined well. The definition of size and position of grain is an advantage for fabrication of electron device such as thin film transistors on controlling grain boundary in a channel region.

No serious defects were observed in crystalline grains. Grain boundaries was formed well defined; no disordered region was observed among crystalline grains. The surface was still smooth after crystallization and the roughness was about 2 nm. These characteristics indicate that the laser crystallized films have good electrical properties with a low density of defects.

On the other hand, amorphization occurs when

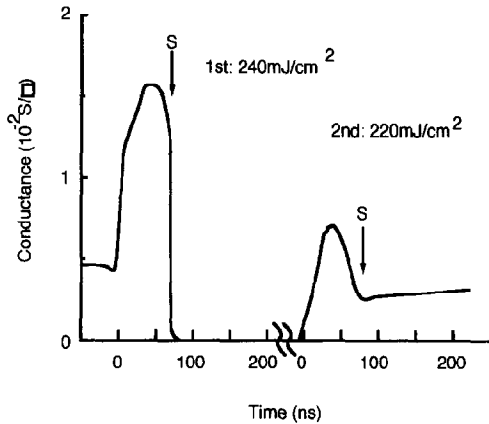


Fig. 2. Electrical Conductance change of 20 nm thick silicon films doped with 2-atomic% phosphorus with irradiation with 2 pulses. 'S' shows a solidification point, which was determined by decrease of optical reflectivity at the silicon surface.

non-patterned silicon films are melted completely. The amorphization threshold energy was much larger than the crystallization threshold energy. The threshold energy for amorphization increased from 195 to 290  $\text{mJ}/\text{cm}^2$  as the film thickness increased from 6 to 36 nm, as shown in Fig. 1. Complete melting of silicon films on a glassy quartz substrate results in a super cooling state because there is few nucleation sites. The liquid silicon can be cooled much below the melting temperature. Very rapid solidification with a high liquid/solid interface velocity is realized because the free energy in liquid silicon in a deep super cooled state is much larger than solid silicon at a solidification temperature [11]. The rapid solidification, which resulted in amorphization, was observed using a transient conductance measurement in the case of amorphization. Fig. 2 shows the conductance as a function of time during and after irradiation for 20 nm thick silicon films doped with 2-atomic% phosphorus. The initial crystallized film was melted followed by amorphized by the first irradiation with a laser energy of 240  $\text{mJ}/\text{cm}^2$ . The conductance due to molten silicon rapidly increased by the irradiation. It rapidly decreased 70 ns after the initiation of melt. The decrease of the conductance was completed within 5 ns (= time resolution). After the termination of melt, the electrical conductivity decreased to  $1 \times 10^{-2}$  S/cm, while the original polycrystalline film had a high electrical conductivity of  $1.5 \times 10^3$

S/cm. This decrease of conductance after solidification means that the silicon film was completely amorphized [12]. The transition from the amorphous state to the crystalline state also occurred when the silicon film was irradiated with a laser energy of 220  $\text{mJ}/\text{cm}^2$ . The electrical conductivity first increased due to melting and gradually decreased after the peak, as shown in Fig. 2. After solidification, the electrical conductivity backed close to the initial value. Crystallization and amorphization of silicon films are reversible. An amorphized silicon can be crystallized again by irradiation with an energy low enough to cause the interface controlled growth.

Silicon films solidifying to the amorphous state is reheated caused by the latent heat, which is released during the rapid solidification of the liquid silicon (recalescence). Crystallization was caused by the recalescence when the film was thicker than 20 nm because the latent heat energy per unit area increases as film thickness increases [13]. On the other hand, complete amorphous films with a high defect density is realized for films thinner than 20 nm. They have a very high electrical conductivity,  $\sim 10^{-3}$  S/cm, characterized as the variable-range hopping conduction with a density of localized states of  $1 \times 10^{20} \text{cm}^{-3} \text{eV}^{-1}$  even in undoped condition.

### 3. TFT fabrication and results

N-channel poly-Si and a-Si TFTs were fabricated using methods of pulsed laser rapid heating with 30 ns pulsed XeCl excimer laser and the  $\text{SiO}_2$  formation methods [5,14–17]. The schematic fabrication processes are shown by Fig. 3, (a) for poly-Si TFTs and (b) for a-Si-TFTs. Islands of 20 nm thick hydrogenated amorphous silicon films doped with 2-atomic% phosphorus were first formed on a glass substrate at 250°C using conventional plasma enhanced chemical vapor deposition (PECVD) and a etching method as dopant sources for forming source and drain regions, as shown in Fig. 3. A 20 nm thick undoped a-Si:H film was then deposited using PECVD over the whole area. Islands patterning was conducted by etching the amorphous layers.

For fabricating the poly-Si TFTs, the silicon layers were crystallized by laser irradiation in vacuum. In order to have a smooth surface by slowly taking

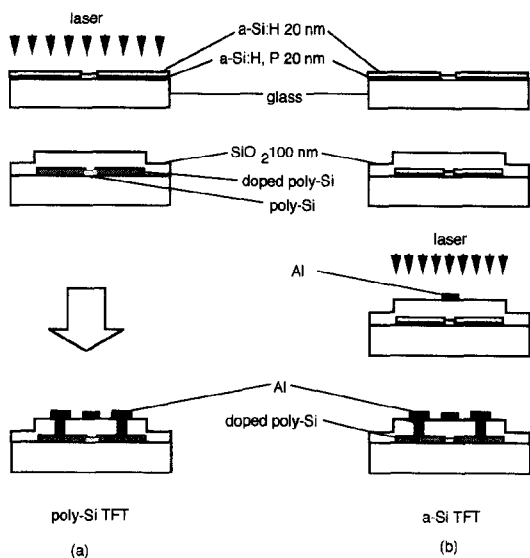


Fig. 3. Schematic fabrication flows of poly-Si (a) and a-Si TFTs (b).

out hydrogen from a film, irradiation with multi energy steps was performed [18]. The laser energy was controlled up to  $230 \text{ mJ/cm}^2$ , which is below the amorphization threshold ( $240 \text{ mJ/cm}^2$ ) for 20 nm thick films. The crystalline films had fine grains with a size of 50 nm at most. The laser heating also caused diffusion of dopant atoms with a diffusion length at most 60 nm from the doped region [19]. The dopant atoms therefore diffuse vertically through the whole thickness of Si layers, but they did not shorten the channel length significantly. After the irradiation, the silicon layers were hydrogenated using hydrogen plasma with 5 W for 30 s at  $270^\circ\text{C}$  in order to reduce defect states [20].

In order to form a  $\text{SiO}_2$  gate insulator layer at a low temperature with low damage, two technologies were developed. One is a triode type remote plasma CVD [15] and the other is  $\text{SiO}$  evaporation with an oxygen ambient [16]. The *remote-plasma-CVD equipment* had mesh electrodes between the top electrode and the substrate in order to confine the plasma and keep it away from the substrate. Mixed gases with oxygen and helium were introduced and their plasma was generated by applying RF voltage to the top electrode. The Langmuir analysis with dependence of current on voltage applied at the

meshes revealed that the electron density was lower than  $10^4 \text{ cm}^{-3}$  in the region between the meshes and the substrate, while the electron density was higher than  $10^9 \text{ cm}^{-3}$  in plasma above the meshes [15]. The oxygen and helium radicals come down in a lower part through the holes in the meshes and decompose  $\text{SiH}_4$  gas which was flowed below the meshes. A  $\text{SiO}_2$  film was consequently formed on a substrate heated at  $270^\circ\text{C}$ . The deposition rate was 6 nm/min at RF power (13.56 MHz) of 5 W. The breakdown voltage was 4.5 MV/cm. The investigation of the Al-gate metal–oxide–silicon (MOS) capacitor using single crystalline silicon revealed that the minimum interface trap density was  $2 \times 10^{10} \text{ cm}^{-2} \text{ eV}^{-1}$  [5]. On the other hand, the interface trap density for a MOS capacitor fabricated using conventional plasma CVD without any mesh was  $7 \times 10^{11} \text{ cm}^{-2} \text{ eV}^{-1}$ .

*SiO evaporation with an oxygen atmosphere* was also used for forming the gate insulator. A powder of  $\text{SiO}$  with a purity of 99.99% put in a Ta boat was evaporated by heating the Ta boat with an oxygen flow. Hot molecular  $\text{SiO}$  evaporated from heated  $\text{SiO}$  powders effectively reacts with oxygen gas so that  $\text{SiO}_2$  films were formed on substrates at room temperature. The deposition rate was controlled 8 nm/min. The deposited film can have a large amount of oxide charge caused by  $E'$  centers (dangling bond of Si in  $\text{SiO}_2$ ) for the deposition condition of a lower oxygen flow rate. The density of the oxide charge is reduced to as small as  $8 \times 10^9 \text{ cm}^{-2}$  by increasing oxygen flow rate to 2.5 Sccm during deposition [21]. The minimum interface trapping density at the mid gap was estimated to be lower than  $1.5 \times 10^{10} \text{ cm}^{-2} \text{ eV}^{-1}$  by measuring the capacitance response as a function of voltage in an Al-gate MOS capacitor. The good interface with the low interface trapping density results from the fact that there are no ions or electrons with a high energy during the film formation. The break down voltage however was 2 MV/cm, which was lower than that of the remote plasma CVD  $\text{SiO}_2$ . After  $\text{SiO}_2$  formation, 100 nm thick Al was then deposited by evaporation and the gate electrodes were defined.

For *fabricating the a-Si TFTs*, the laser irradiation was carried out after the formation of the Al gate metal in order to form doped poly-Si source and drain regions with a resistivity of  $1 \times 10^3 \Omega \text{ cm}$  and to keep the channel region the amorphous state by

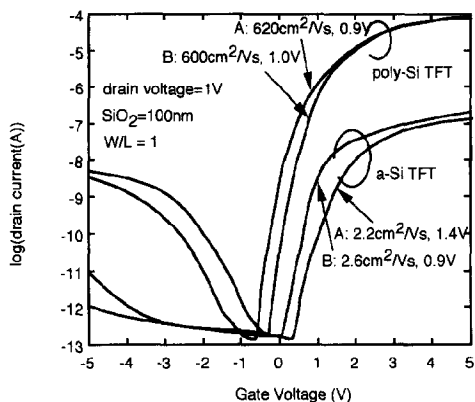


Fig. 4. The transfer characteristics for poly-Si and a-Si TFTs. 'A' shows TFTs with SiO<sub>2</sub> fabricated using remote plasma and 'B' shows TFTs with SiO<sub>2</sub> fabricated using evaporation. The maximum field effect mobility and threshold voltage are presented.

reflecting the laser light with the Al gate, as shown in Fig. 3(b).

Contact holes were opened in the SiO<sub>2</sub> layers at the source and drain regions for both TFTs. The Al source and drain electrodes were formed using evaporation and lift-off methods. After the fabrication, poly-Si and a-Si TFTs were annealed at 270°C for 1 hr in H<sub>2</sub>O vapor atmosphere, in order to improve properties of SiO<sub>2</sub> and the SiO<sub>2</sub>/Si [22].

Fig. 4 shows the transfer characteristics for the poly-Si TFTs and a-Si TFTs, respectively. The TFTs had low threshold voltages from 0.9 to 1.4 V. The density of trapping states in the TFT was estimated with the sub-threshold slope of the transfer characteristics neglecting the component of capacitance caused by a depletion region because the thickness of the Si films in the channel region was very thin (20 nm) [5,23]. The poly-Si TFTs and a-Si TFTs have similar defect density ( $2 \sim 3.5 \times 10^{11} \text{ cm}^{-2} \text{ eV}^{-1}$ ). The maximum field effect mobility was 620 cm<sup>2</sup>/Vs at around 1 V above the threshold voltage for the poly-Si TFTs and 2.6 cm<sup>2</sup>/Vs for the a-Si TFTs.

So far, it has been recognized that polycrystalline films with a large grain is essential to fabricate poly-Si TFTs with a high mobility. However, the results of Fig. 4 show two important points. One is that crystalline films fabricated by the laser melting method have good electronic properties with a high mobility even if the films have grains smaller than

100 nm. The other is that the formation of the insulator/Si is essential to fabricate good TFTs. Formation of the interface with low damage is important for TFTs. a-Si TFTs had the high field effect mobilities and the low threshold voltages as well as poly-Si TFTs, as shown in Fig. 4. This means that there is still a damage problem in conventional fabrication process of a-Si TFTs using plasma CVD.

#### 4. Application of laser ablation

Laser ablation has been widely studied to form films of insulator, semiconductor and superconductor materials. Moreover, it has been also investigated for fine patterning. Laser ablation is an attractive technique for TFT processing. Especially, film formation is expected at low temperature. We have recently tried a kind of laser ablation, so called laser-induced forward transfer, to form thin films. Similar technologies have been already reported by some researchers [24]. The point of our method is the usage of a layer containing volatile atoms in the layer, which can be evaporated by laser heating. An Al film was formed both on an a-Si:H layer which have a hydrogen atoms with a concentration of 10 atomic% and on poly-Si region with no hydrogen, which was fabricated by laser irradiation, as shown in Fig. 5. XeCl excimer laser with an energy of 200 mJ/cm<sup>2</sup> was irradiated to the films from the rear side of the transparent glass substrate. Only Al layer formed on the a-SiH was removed as shown by an inset photograph in Fig. 5 and attached to another substrate positioned in front of the sample. After the irradiation, the amorphous silicon film was not destroyed and kept the smooth surface. On the other hand, the Al layer formed on the poly-Si was not removed. These phenomena are interpreted as follows. When the silicon film is rapidly heated by the laser irradiation, the evaporation pressure of hydrogen in the a-Si:H film increases. The Al film can be removed by the high pressure of hydrogen evaporating from the a-Si:H and attached to the substrate facing the sample. On the other hand, Al formed on the poly-Si is not removed because there is no evaporative species. Although the poly-Si film was also heated by the irradiation, the energy is too low to ablate poly-Si or Al films directly. This result of Fig. 5

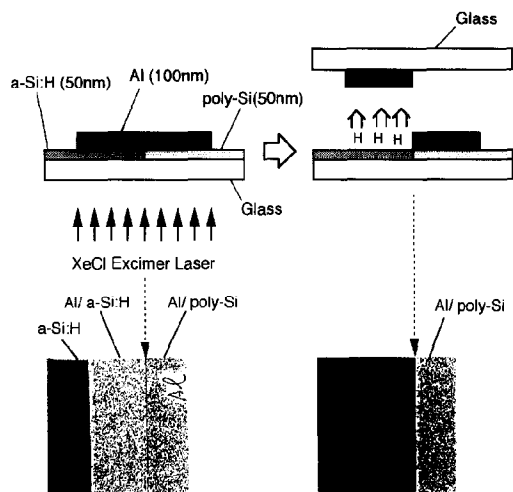


Fig. 5. Schematic experiment of laser-induced forward transfer of an Al layer using an 50 nm thick a-Si:H layer with 10 atomic% hydrogen atoms. A 50 nm thick polycrystallized silicon without hydrogen was also used for comparison. Insets are photographs of the sample before and after irradiation.

shows evaporation of hydrogen has a role for removing an overlying layer at a low laser energy. The present method may be useful for forming metal electrodes for TFT fabrication. Moreover, it would make a new and simple fabrication process possible. For example, TFTs could be directly transferred into an every display pixel as a switching element in a panel with a large size for LCD from a source of TFTs, which are fabricated with a high packing density on another substrate coated with an appropriate film with volatile atoms. The process steps and the tact time for forming TFTs on the display panel could be reduced using this system. Since TFT is very small compared with a display element in general, a small substrate can be used for the preparation of dense TFTs. It allows a very fine and precise design rule although it is still difficult to fabricate very small TFTs on a large substrate.

## 5. Summary

Pulsed laser melt-regrowth of silicon films formed on a quartz substrate provides solidification modes of crystallization and amorphization. Poly-Si films with fine crystalline grains ( $< 100$  nm) and a smooth

surface were formed by the interface controlled growth with a velocity of 0.6 m/s by a XeCl excimer laser irradiation. Large grain growth ( $> 1$   $\mu\text{m}$ ) was achieved by many pulses irradiation, explosive crystallization and by temperature gradient induced in the lateral direction via change in the film shape. On the other hand, an amorphous state was realized via rapid solidification when silicon films were melted completely. Crystallization and amorphization are reversible. They were governed by the laser energy density.

Top-gate-type poly-Si (fine grain) and a-Si TFTs were fabricated at 270°C using technologies of laser crystallization and methods of  $\text{SiO}_2$  formation in remote plasma chemical vapor deposition or SiO evaporation with an oxygen ambient. The maximum field effect mobility was 620  $\text{cm}^2/\text{Vs}$  for poly-Si TFTs and 2.6  $\text{cm}^2/\text{Vs}$  for a-Si TFTs. The low threshold voltage were 0.85 ~ 1.4 V for both TFTs. These results demonstrate that TFT can have good performances by forming  $\text{SiO}_2$  gate insulator with low damage.

Application of a laser-induced-forward transfer to TFT fabrication was proposed. An Al film was removed and transferred by heating an a-Si:H film and evaporating hydrogen gas from the silicon film, on which the Al was formed. It may have a possibility to establish a simple fabrication process with a low cost.

## Acknowledgements

The author would like to acknowledge M. Sekiya, M. Hara, N. Sano, and A. Kohno for experiments and helpful discussions. He also thanks Dr. T. Yamada and Prof. H.-J. Queisser for their support.

## References

- [1] T. Sameshima, S. Usui and M. Sekiya, IEEE Electron Device Lett. EDL-7 (1986) 276.
- [2] K. Sera, F. Okumura, H. Uchida, S. Itoh, S. Kaneko and K. Hotta. IEEE Trans. Electron Devices 36 (1989) 2868.
- [3] T. Serikawa, S. Shirai, A. Okamoto and S. Suyama, Jpn. J. Appl. Phys. Lett. 28 (1989) 1871.
- [4] H. Kuriyama, T. Kuwahara, S. Ishida, T. Nohda, K. Sano, H. Iwata, S. Noguchi, S. Kiyama, S. Tsuda, S. Nakano, M. Osumi and Y. Kuwano, Jpn. J. Appl. Phys. 31 (1992) 4550.

- [5] A. Kohno, T. Sameshima, N. Sano, M. Sekiya and M. Hara, *IEEE Trans. Electron Devices* 42 (1995) 251.
- [6] T. Sameshima, M. Hara and S. Usui, *Jpn. J. Appl. Phys.* 29 (1990) 548.
- [7] T. Sameshima, M. Hara and S. Usui, *Jpn. J. Appl. Phys.* 29 (1990) 1363.
- [8] H. Kuriyama, T. Nohda, Y. Aya, T. Kuwahara, K. Wakisaka, S. Kiyama and S. Tsuda, *Jpn. J. Appl. Phys.* 33 (1992) 5657.
- [9] J.S. Im and H.J. Kim, *Appl. Phys. Lett.* 64 (1994) 2303.
- [10] T. Sameshima, *Jpn. J. Appl. Phys. Lett.* 32 (1993) 1485.
- [11] S.R. Stiffler, P.V. Evans and A.L. Greer, *Acta Met. Mater.* 40 (1992) 1617.
- [12] T. Sameshima and S. Usui, *J. Appl. Phys.* 70 (1991) 1281.
- [13] T. Sameshima and S. Usui, *Appl. Phys. Lett.* 59 (1991) 2724.
- [14] M. Sekiya, M. Hara, N. Sano, A. Kohno and T. Sameshima, *IEEE Electron Device Lett.* EDL-15 (1994) 69.
- [15] N. Sano, A. Kohno, M. Hara, M. Sekiya and T. Sameshima, *Appl. Phys. Lett.* 65 (1994) 162.
- [16] T. Sameshima, A. Kohno, M. Sekiya, M. Hara, N. Sano, *Appl. Phys. Lett.* 64 (1994) 1018.
- [17] T. Sameshima, A. Kohno, M. Sekiya, M. Hara and N. Sano, *Jpn. J. Appl. Phys. Lett.* 33 (1994) 834.
- [18] T. Sameshima, M. Hara and S. Usui, *Jpn. J. Appl. Phys.* 28 (1989) 1789.
- [19] T. Sameshima and S. Usui, *Jpn. J. Appl. Phys. Lett.* 26 (1987) 1208.
- [20] T. Sameshima, M. Sekiya, M. Hara, N. Sano and A. Kohno, *J. Appl. Phys.* 76 (1994) 7377.
- [21] T. Sameshima and G. Langguth, *J. Appl. Phys.*, submitted.
- [22] N. Sano, A. Kohno, M. Hara, M. Sekiya and T. Sameshima, *Appl. Phys. Lett.*, submitted.
- [23] S.M. Sze, *Physics of Semiconductor Devices*, 2nd ed. (Wiley, New York, 1981) ch. 8.
- [24] E. Fogarassy, C. Fuchs, F. Kerherve, G. Hauchecorne and J. Perrière, *J. Mater. Res.* 4 (1989) 1082.